JOC Article

Transformation of α-Tocopherol (Vitamin E) and Related Chromanol Model Compounds into Their Phenoxonium Ions by Chemical Oxidation with the Nitrosonium Cation

Stephen B. Lee, Ching Yeh Lin, Peter M. W. Gill, and Richard D. Webster*

Research School of Chemistry, Australian National University, Canberra ACT 0200, Australia

webster@rsc.anu.edu.au

Received August 26, 2005

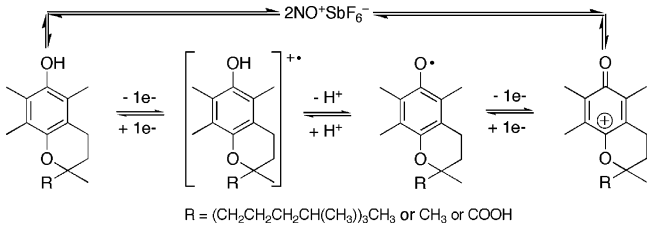

α-Tocopherol (α-TOH), the main oil component making up vitamin E, and its nonnatural solid 6-hydroxy-2,2,5,7,8-pentamethylchroman and 6-hydroxy-2,5,7,8-tetramethylchroman-2-carboxylic acid structurally related analogues were oxidized quantitatively with 2 mol equiv of $NO^+SbF_6^-$ in CH_3CN at 233 K to form phenoxonium cations (α-$TO^+SbF_6^-$) in a chemically reversible two-electron/one-proton process. Solution-phase infrared spectroscopy, ^1H and ^{13}C NMR spectroscopy, and corresponding theoretical calculations of the spectroscopic data using density-based and wave-function-based models support the identity of the remarkably stable phenoxonium cations. The presence of an oxygen atom in the para position to the hydroxyl group and the chromanol ring structure appear to be important factors in stabilization of the phenoxonium ions, which raises the interesting possibility that the cations play a crucial role in the mode of action of vitamin E in biological systems. Although the phenoxonium cations are reactive toward nucleophiles such as water, they may be moderately stable in the hydrophobic (lipophilic) environment where vitamin E is known to occur naturally.

1. Introduction

α-Tocopherol (α-TOH) is the most naturally abundant, fully methylated, and biologically active of the four (α, *β*, *γ*, and *δ*) structurally related phenolic lipophilic compounds that are labeled vitamin E. α-TOH is thought to play an important role as an antioxidant in mammalian tissues by inhibiting the free radical chain autooxidation of polyunsaturated fatty acid esters (LH) in two principal steps.[1] First, α-TOH reacts with an oxidized site on a lipid cell wall (LOO•) to yield a molecule of lipid hydroperoxide (LOOH) and the tocopheroxyl radical (α-TO•). Second, the α-TO• radical reacts with another LOO• radical so that, overall, one α-TOH molecule is able to inhibit two LOO• sites. The localization and mobility of α-TOH within the lipids are critical to its ability to function, as well as are synergistic interactions with other species such as ascorbic acid, hydroquinones, and catechols.[1d,g] In addition to vitamin E sacrificially preventing cell damage, there is evidence that it may function instead, or as well, by a mechanism that is not directly related to the inhibition of oxidation[2] and has a different function in mammals and plants.[3] To date, the important biological chemistry of vitamin E is thought to involve only the neutral compound (α-TOH) and its related phenoxyl radical (α-TO•). Nevertheless, voltammetry experiments[4,5] have demonstrated the existence

* Fax: + 61 2 6125 0750.

(1) The following recent citations are representative examples of the numerous reviews describing the mechanisms of inhibition of lipid peroxidation by vitamin E. (a) Packer, L.; Witt, E. H.; Tritschler, H. J. *Free Radical Biol. Med.* **1995**, *19*, 227−250. (b) Bowry, V. W.; Ingold, K. U. *Acc. Chem. Res.* **1999**, *32*, 27−34. (c) Traber, M. G.; Arai, H. *Annu. Rev. Nutr.* **1999**, *19*, 343−355. (d) Wang, X.; Quinn, P. J. *Prog. Lipid Res.* **1999**, *38*, 309−336. (e) Finkel, T.; Holbrook, N. J. *Nature* **2000**, *408*, 239−247. (f) Wang, X.; Quinn, P. J. *Mol. Membr. Biol.* **2000**, *17*, 143−156. (g) Niki, E.; Noguchi, N. *Acc. Chem. Res.* **2004**, *37*, 45−51.

(2) For example, see: (a) Azzi, A.; Stocker, A. *Prog. Lipid Res.* **2000**, *39*, 231−255. (b) Ricciarelli, R.; Zingg, J.-M.; Azzi, A. *Biol. Chem.* **2002**, *383*, 457−465. (c) Azzi, A.; Ricciarelli, R.; Zingg, J.-M. *FEBS Lett.* **2002**, *519*, 8−10.

(3) Munne-Bosch, S.; Alegre, L. *Crit. Rev. Plant Sci.* **2002**, *21*, 31−57.

10.1021/jo0517951 CCC: $30.25
Published on Web 11/16/2005

SCHEME 1. Electrochemically Induced Transformations of α-Tocopherol[a,b]

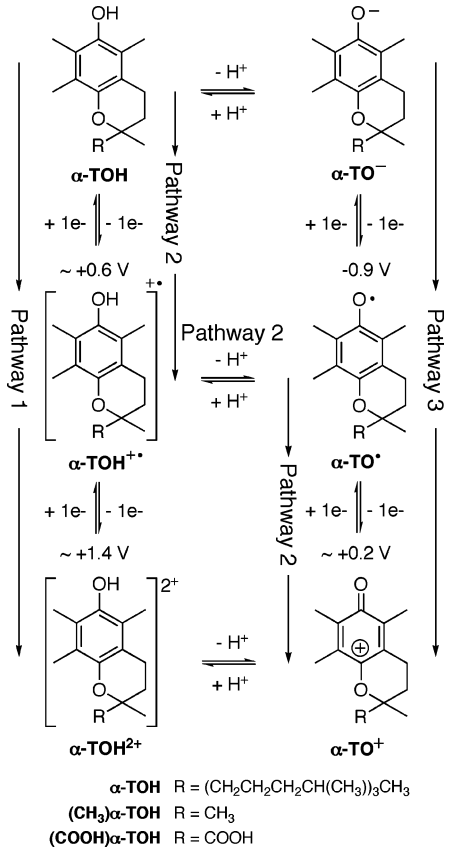

[a] Refs 4 and 7. [b]One resonance structure is displayed for each compound. The listed potentials (vs Fc/Fc^+) were obtained by voltammetry and are the approximate values necessary to bring about oxidation of the phenolic compounds but do not necessarily correspond to the formal potential. The counterions for the charged species are the supporting electrolyte cation [Bu_4N^+] and anion [PF_6^-].

of several other forms of α-tocopherol that are easily electrochemically accessible through proton and electron transfers (Scheme 1). The phenoxonium closed-shell cation (α-TO^+) that will be described in more detail here has recently been found to be surprisingly stable under mild conditions in solution (a dry aprotic organic solvent), although evidence for its existence has been restricted to infrared and UV−vis spectroscopies.[4] Phenoxonium cations are thought to be critical intermediates in oxidation processes associated with phenols but are usually very unstable, with few reports of compounds stable enough to characterize.[6] Therefore, it is a significant observation that the phenoxonium cation derived from a naturally occurring compound is stable in solution.

In acetonitrile, at approximately neutral pH, α-TOH can be electrochemically oxidized by one electron at solid electrodes to form the cation radical (α-$TOH^{+\bullet}$). α-$TOH^{+\bullet}$ quickly dissociates into α-$TO^\bullet$ (and H^+), which is immediately further oxidized at the electrode surface by one electron to form the brightly orange/red- ($\lambda_{max} = 452$ nm; $\epsilon = 2.5 \times 10^3$ L cm^{-1} mol^{-1})[4] colored α-TO^+ (Scheme 1, pathway 2). α-TO^+ is stable for at least several hours at low temperatures and can be reduced back to α-TOH on both the cyclic voltammetry (seconds) and the controlled potential electrolysis (CPE) (hours) timescales,[4b] although it is unstable in the presence of nucleophiles and has been reported to react with water/moisture to form 9-hydroxy-α-tocopherone (**1**), which slowly rearranges to the quinone (**2**) (eq 1).[8] The addition of an equimolar amount of

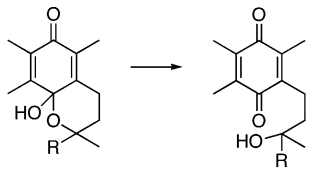

(1)

organo-soluble base (such as Et_4NOH) to solutions of α-TOH immediately forms the phenolate anion (α-TO^-),[5] which can be oxidized in two sequential one-electron steps to also form α-TO^+ (Scheme 1, pathway 3). In the presence of ~≥1−2% CF_3SO_3H (or another organo-soluble acid[4a]), α-TOH is oxidized in two sequential one-electron steps to form α-$TOH^{+\bullet}$ first and then, at more positive potentials, the dication (α-TOH^{2+}) is most likely formed (Scheme 1, pathway 1).[4]

Although electrooxidation of α-TOH is a proven pathway to the α-TO^+ cation in high yield in CH_3CN,[4] it requires at least a 30-fold excess of supporting electrolyte to avoid the effects of migration, which otherwise results in the charged species produced in the working electrode compartment moving to the counter electrode compartment and reacting irreversibly with species produced at the auxiliary electrode.[9] We were interested in testing the stability of α-TO^+ under low ionic strength conditions, closer to those encountered in a lipophilic environment, and in testing whether the cation could form by a homogeneous electron-transfer mechanism in addition to the heterogeneous reactions at solid electrodes. NO^+ was chosen as the chemical oxidant because it has a reduction potential of +0.87 V vs Fc/Fc^+ in CH_3CN,[10] which exceeds the oxidation potential of the phenols by at least ~+0.3−0.4 V, and because it is easily obtained as high-purity dry salts. Furthermore, NO^+ is useful as an in situ oxidant because it is NMR (^1H and ^{13}C) silent and because its reduced form is easily removed from solution as a gaseous product. The closely related higher melting point

(4) (a) Svanholm, U.; Bechgaard, K.; Parker, V. D. *J. Am. Chem. Soc.* **1974**, *96*, 2409−2413. (b) Williams, L. L.; Webster, R. D. *J. Am. Chem. Soc.* **2004**, *126*, 12441−12450.

(5) (a) Nanni, E. J., Jr.; Stallings, M. D.; Sawyer, D. T. *J. Am. Chem. Soc.* **1980**, *102*, 4481−4485. (b) Webster, R. D. *Electrochem. Commun.* **1999**, *1*, 581−584.

(6) (a) Speiser, B.; Rieker, A. *J. Chem. Res. (S)* **1977**, 314−315. (b) Vigalok, A.; Rybtchinski, B.; Gozin, Y.; Koblenz, T. S.; Ben-David, Y.; Rozenberg, H.; Milstein, D. *J. Am. Chem. Soc.* **2003**, *125*, 15692−15693.

(7) For comprehensive reviews on the anodic electrochemistry of phenols, see: (a) Yoshida, K. *Electrooxidation in Organic Chemistry. The Role of Cation Radicals as Synthetic Intermediates*; Wiley: New York, 1983; pp 174−186. (b) Hammerich, O.; Svensmark, B. In *Organic Electrochemistry*, 3rd ed.; Lund, H., Baizer, M. M., Eds.; Marcel Dekker: New York, 1991; Chapter 16. (c) Rieker, A.; Beisswenger, R.; Regier, K. *Tetrahedron* **1991**, *47*, 645−654. (d) Eickhoff, H.; Jung, G.; Rieker, A. *Tetrahedron* **2001**, *57*, 353−364.

(8) (a) Dürckheimer, W.; Cohen, L. A. *J. Am. Chem. Soc.* **1964**, *86*, 4388−4393. (b) Marcus, M. F.; Hawley, M. D. *J. Org. Chem.* **1970**, *35*, 2185−2190.

(9) The supporting electrolyte also lowers the solution resistance to enable electrolysis to be performed in organic solvents with low dielectric constants.

(10) (a) Kochi, J. K. *Acc. Chem. Res.* **1992**, *25*, 39−47. (b) Connelly, N. G.; Geiger, W. E. *Chem. Rev.* **1996**, *96*, 877−910.

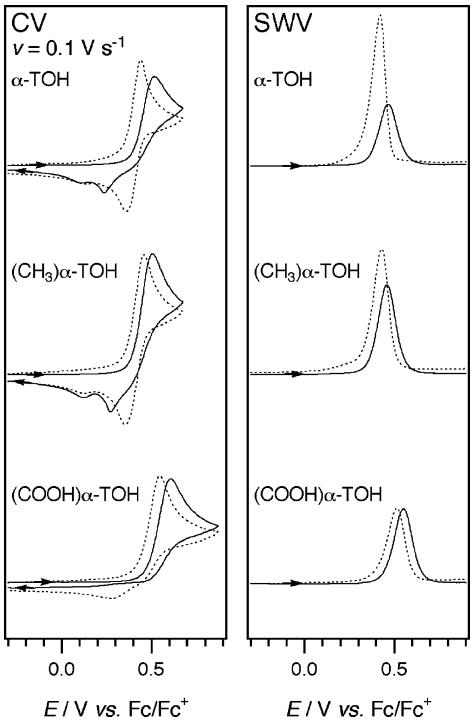

FIGURE 1. Voltammetric data for 2 mM substrates obtained at 293 K in CH_3CN with 0.2 M Bu_4NPF_6 at 1 mm diameter planar Pt (—) and GC (- - -) electrodes.

nonnatural compounds 6-hydroxy-2,2,5,7,8-pentamethylchroman [(CH_3)α-TOH] and 6-hydroxy-2,5,7,8-tetramethylchroman-2-carboxylic acid [(COOH)α-TOH] (Scheme 1) were also tested.

2. Results and Discussion

2.1. Mechanistic Considerations Derived From Voltammetry Experiments. Cyclic (CV) and square wave (SWV) voltammograms of α-TOH, (CH_3)α-TOH, and (COOH)α-TOH in CH_3CN at 293 K are shown in Figure 1. The voltammograms are more complicated than expected for a simple reversible electron transfer because they are affected by homogeneous reactions and surface-based interactions of the solutes with the electrodes[4b] and are associated with the pathway 2 series of electron transfers and the homogeneous reaction given in Scheme 1. In each case, the peak values on the forward scan direction for both CV and SWV experiments are at less positive potentials on GC compared to those on Pt. Because the potential of the voltammetric wave is influenced by the kinetics of the homogeneous reactions, the peak potentials (or half-wave potentials) do not correspond to the thermodynamic formal potentials ($E°$). The SWV shows larger anodic peak currents on GC compared to those on Pt (especially for α-TOH), which is thought to be associated with a rapid adsorption/desorption process on GC.[4b] The anodic peak currents observed for (COOH)α-TOH appeared to be the same on Pt and GC electrodes, suggesting less surface-based interactions compared to (CH_3)α-TOH and α-TOH.

The CVs observed for α-TOH and (CH_3)α-TOH at the same electrode and temperature were very similar, indicating that the mechanism and kinetics of oxidation were also likely to be very similar and unaffected by the replacement of the phytyl group in α-TOH with a methyl group in (CH_3)α-TOH. The anodic peak current was slightly less for α-TOH because of a smaller diffusion coefficient brought about by the bulky phytyl chain. The anodic−cathodic peak-to-peak separation (ΔE_{pp}) was smaller on GC compared to that on Pt, although the peak shapes on both electrodes were complicated. As the temperature was lowered, the ΔE_{pp} values increased substantially, far more than can be accounted for by the effects of uncompensated resistance. The voltammogram for (COOH)α-TOH showed only a small reverse peak on the cyclic voltammetry timescale, which might be caused by less chemical reversibility (at $T = 293$ K) compared to the other phenols.

Digital simulation techniques allowed approximate kinetic parameters to be calculated for the electrochemically induced oxidation reaction of α-TOH to produce α-TO^+ that is represented through the reversible series of steps given in eqs 2−4 (Scheme 1, pathway 2). Simulations were performed on the data obtained at 243 K (Figure 2) because CPE experiments had previously indicated that at this temperature the chemical transformations were completely reversible (at higher temperatures, this might not be the case).[4b]

$$\text{α-TOH} - e^- \rightleftarrows \text{α-TOH}^{+\bullet}$$
$$E° = +0.55 \text{ V}; k_s = 0.005 \text{ cm s}^{-1} \quad (2)$$

$$\text{α-TOH}^{+\bullet} \rightleftarrows \text{α-TO}^{\bullet} + H^+$$
$$K_{eq} = 1 \times 10^{-7} \text{ mol L}^{-1};$$
$$k_f = 1 \times 10^3 \text{ s}^{-1}; k_b = 1 \times 10^{10} \text{ L mol}^{-1} \text{ s}^{-1} \quad (3)$$

$$\text{α-TO}^{\bullet} - e^- \rightleftarrows \text{α-TO}^+$$
$$E° = +0.13 \text{ V}; k_s = 0.005 \text{ cm s}^{-1} \quad (4)$$

$$\text{α-TO}^{\bullet} + \text{α-TO}^{\bullet} \rightleftarrows \text{products}$$
$$K_{eq} = 1 \times 10^4 \text{ L mol}^{-1};$$
$$k_f = 1 \times 10^3 \text{ L mol}^{-1} \text{ s}^{-1}; k_b = 1 \times 10^{-1} \text{ s}^{-1} \quad (5)$$

The reversibility of the complete electrochemical transformation (eqs 2−4) is critically determined by the equilibrium constant for the proton dissociation reaction in eq 3 because the K_{eq} value must be sufficiently low to enable the back-reaction to occur on the voltammetric timescale. The values of the homogeneous rate constants in eq 3 are also very important because α-$TO^{\bullet}$ is not stable in solution and decays by a bimolecular self-reaction (eq 5).[11] Therefore, the backward transformation step in eq 3 must be faster than the forward bimolecular self-reaction in eq 5, otherwise α-$TO^{\bullet}$ would react before it was further oxidized to the phenoxonium ion. The k_f value in eq 5 was previously calculated over a range of temperatures by simulation of CV data obtained during the oxidation of the phenolate anion (α-TO^-) in CH_3CN.[5b] The K_{eq}, k_f, and k_b values in eq 3 were estimated from CV experiments with the addition of varying concentrations of CF_3SO_3H because the addition of acid shifts the equilibrium toward the protonated species (Figure 2)

(11) Bowry, V. W.; Ingold, K. U. *J. Org. Chem.* **1995**, *60*, 5456−5467.

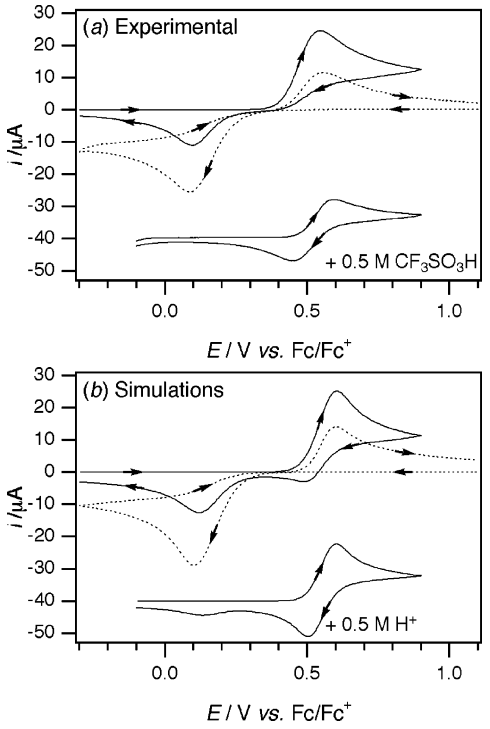

FIGURE 2. (a) Cyclic voltammograms of 15 mM substrates recorded in CH_3CN with 0.5 M Bu_4NPF_6 at a 1 mm diameter planar Pt working electrode at 243 K. The CV recorded in the presence of 0.5 M CF_3SO_3H is offset by −40 μA. α-TOH (—). α-TO^+ (- - -), synthesized by exhaustive two-electron oxidation of α-TOH in a controlled potential electrolysis cell. (b) DigiSim simulations of the experimental data in (a), using the parameters given in eqs 2−5, with a solution resistance of 600 Ω. The CV simulated in the presence of 0.5 M H^+ is offset by −40 μA.

(CF_3SO_3H was assumed to fully dissociate in CH_3CN). At concentrations of acid above ca. 0.5 M, the forward electrochemical transformation mainly produces α-$TOH^{+\bullet}$, which can be reduced back to the starting material when the scan direction is reversed; hence, the CV appears similar to what is expected for a simple reversible electron transfer (Figure 2). Simulations were also performed on CV data obtained in solutions of α-TO^+ (from the bulk oxidation of α-TOH) that aided the estimation of the kinetic parameters (Figure 2, dashed lines). The rate and equilibrium constants in eq 2−5 are specific for CH_3CN at 243 K and are possibly quite different in lower dielectric media like CH_2Cl_2 (see below) and at higher temperatures. Importantly, the simulations confirm that the back-reaction in eq 3 is fast and the equilibrium constant is very low, which is the reason the transformation from phenol to a phenoxonium cation occurs readily in both directions in CH_3CN.

2.2. FTIR Spectroscopy. The chemical oxidation reactions were performed at 233 K and monitored with in situ attenuated total reflection Fourier transform infrared (ATR-FTIR) spectroscopy. Oxidation of the three phenols with 2 mol of NO^+ (eq 6) produced dark green

$$\text{α-TOH} \xrightleftharpoons[\text{CH}_3\text{CN}]{2\text{NO}^+\text{SbF}_6^-} \text{α-TO}^+\text{SbF}_6^- + [\text{CH}_3\text{CNH}]^+\text{SbF}_6^- + 2\text{NO}_{(g)} \quad (6)$$

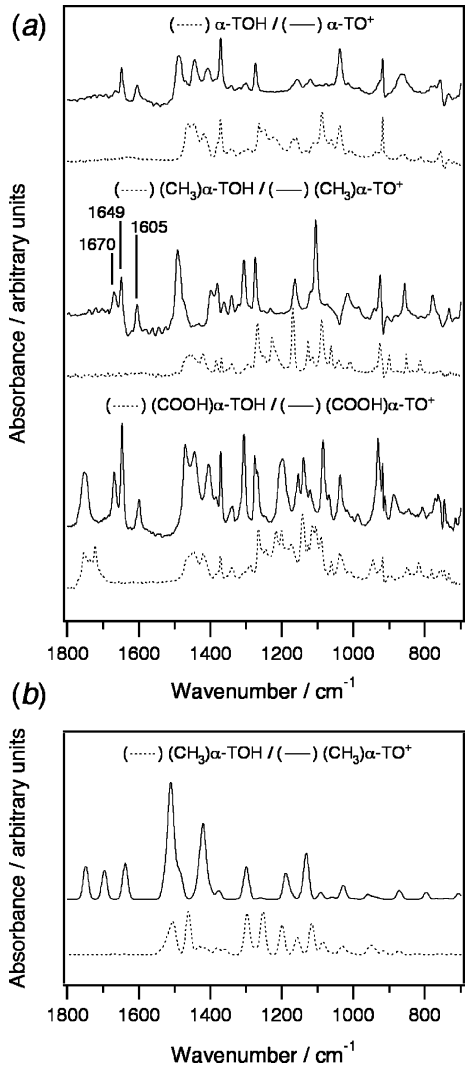

FIGURE 3. (a) Background subtracted solution-phase ATR-FTIR spectra obtained at 233 K in CH_3CN with between 15 and 40 mM phenols before (···) and after (—) the addition of 2 mol equiv of $NOSbF_6$ to form the phenoxonium cations. Each spectrum represents 128 accumulated scans recorded at 2 cm^{-1} resolutions. (b) Theoretical infrared spectra calculated at the EDF2/6-31+G* level.

solutions that within 2−3 min transformed into bright orange/red solutions (Supporting Information Figure S1) with very similar IR spectra between 1500 and 1800 cm^{-1} (Figure 3a, solid lines), indicating the formation of the phenoxonium ions in high yields.[4b] Also consistent with the formation of the phenoxonium cations was the observation that the strong OH stretches in the FTIR spectra of the phenolic starting materials at ca. 3400 cm^{-1} were missing from the spectrum of the oxidized compounds.[12]

The "H^+" released during oxidation of the phenol probably exists coordinated to the solvent and weakly ion paired with the SbF_6^- anion (eq 6). In addition to the bands detected at 1605 and 1649 cm^{-1}, (CH_3)α-TO^+ and (COOH)α-TO^+ showed a strong band at 1670 cm^{-1}, which was also present in the spectrum of α-TO^+ but was of

(12) Pouchert, C. J. *The Aldrich Library of FT-IR Spectra*, 1st ed.; Aldrich Chemical Co., Inc.: Milwaukee, WI, 1985; Vol. 1, pp 452−457.

lower intensity and so was not highlighted in an earlier study that used electrolysis procedures to generate α-TO^+.[4b] (COOH)α-TOH and (COOH)α-TO^+ showed extra bands at ~1750 cm^{-1} due to the presence of the carboxylic acid functional group. In each case, the spectra of the oxidized compounds and the solution color remained constant over a period of at least 2 h (at 233 K), indicating substantial stability of the phenoxonium cations.

When 200 mM of water was added to the solutions containing the phenoxonium cations at 233 K, the color faded from bright orange/red to pale yellow over a period of approximately 10 min. During the color change, the infrared peaks at 1605, 1649, and 1670 cm^{-1} disappeared completely while a new band appeared at 1641 (oxidized α-TOH and (CH_3)α-TOH) or 1645 cm^{-1} (oxidized (COOH)α-TOH). The spectroscopic results indicate that a transformation occurs in the presence of relatively low levels of water with the strong absorbance at 1641 or 1645 cm^{-1}, indicating the formation of new carbonyl-containing compound(s) (such as **1** or **2** in eq 1).

Chemical oxidation experiments were also performed on 2,4,6-tri-*tert*-butylphenol and 2,6-di-*tert*-butyl-4-methoxyphenol, two compounds that are known to form stable phenoxyl radicals.[13] Oxidation of 2,4,6-tri-*tert*-butylphenol at 233 K produced darkly colored solutions that became pale yellow within 1 min. A strong band at 1656 cm^{-1} did not change when water was added, suggesting that it was associated with a relatively stable product but not a phenoxonium cation (the rapid color change also suggested that the phenoxonium cation quickly decomposed, if it actually formed). Oxidation of 2,6-di-*tert*-butyl-4-methoxyphenol produced a darkly colored solution that transformed to an orange/red color and then within 5 min faded to a pale yellow color. In situ ATR-FTIR spectroscopy detected transitory absorbancies at 1640 and 1575 cm^{-1} that diminished as the orange/red color faded, which is consistent with the presence of a phenoxonium cation, albeit of limited stability (Supporting Information Figure S2). The final pale yellow solution had strong bands at 1655 and 1602 cm^{-1}, consistent with a stable species with a quinone structure. It is possible that the oxygen atom in the para position to the carbonyl group aids in the stabilization of the phenoxonium cations, but other factors must also be involved to account for the high stability of the phenoxonium cation of vitamin E and its analogues compared to only limited suggested stability of the 2,6-di-*tert*-butyl-4-methoxyphenoxonium cation.

When the solvent was removed from solutions containing the (CH_3)α-TO^+ and (COOH)α-TO^+ cations at 243 K with a diffusion pump ($p = 1 \times 10^{-5}$ mmHg), red solid materials were obtained that consisted of the phenoxonium cation and acid (eq 6). The solid material could be handled in a drybox at room temperature and appeared stable for around 24 h, although it became sticky and changed to a much darker red color with increasing time. Infrared spectra of the fresh solid compounds showed bands at 1670, 1649, and 1605 cm^{-1}, indicating that the phenoxonium cations were semistable at room temperature in the solid state (Supporting Information Figure S3) and that the infrared spectra in the carbonyl region were not influenced by solvation effects.

Theoretical infrared spectra were calculated for (CH_3)α-TOH and (CH_3)α-TO^+ (Figure 3b) using the EDF2/6-31+G* model. The unscaled theoretical spectrum of the starting material showed no absorbancies above 1600 cm^{-1} and showed several strong absorbancies between 1550 and 1100 cm^{-1} that coincided reasonably well with the experimental spectrum, albeit shifted to higher wavenumbers by approximately 50 cm^{-1}. The calculations predicted three new strong bands between 1800 and 1600 cm^{-1} in the theoretical spectrum of the cation, which correlate with three strong bands observed in the experimental spectrum of (CH_3)α-TO^+, although with closer spacing between the bands. The theoretical absorptions correspond to a C=O stretch, a symmetric C=C ring stretch, and an asymmetric C=C ring stretch, from highest to lowest wavenumber, respectively. (Ball-and-stick diagrams showing the stretching modes are given in Supporting Information Figure S4.) It is possible that the highest intensity absorption observed in the experimental spectrum at 1649 cm^{-1} is associated with the carbonyl stretch, whereas the relatively weaker bands at 1670 and 1605 cm^{-1} are due to the C=C ring symmetric and asymmetric stretching modes, respectively.

2.3. NMR Spectroscopy. ^1H and ^{13}C NMR experiments were conducted on oxidized solutions of (CH_3)α-TOH in CD_3CN at 233 K because the high solubility minimized the required ^{13}C NMR spectral collection times, compared to those for α-TOH and (COOH)α-TOH, and decreased the likelihood of decomposition occurring. Furthermore, the presence of two methyl groups in (CH_3)α-TO^+ removes the chirality at the quaternary carbon and simplifies the ^1H NMR spectra (compared to those of (COOH)α-TO^+ and α-TO^+) and the absence of the phytyl chain simplifies the ^{13}C NMR spectrum compared to that of α-TO^+. Both the ^1H and the ^{13}C NMR spectra of (CH_3)α-TO^+ (Figure 4) were very clean and free of any decomposition products, indicating that the chemical oxidation occurs quantitatively and that the oxidized products were completely stable in solution on the timescale of the experiment (several hours). The ^1H NMR line width of (CH_3)α-TO^+ was greater than that of (CH_3)α-TOH (Figure 4) which was most likely caused by the presence of a small amount of the (CH_3)α-$TOH^{+\bullet}$ radical. Previous in situ electrochemical-NMR (^1H) experiments performed during the oxidation of α-TOH using a 10 nm thick Au film working electrode positioned within the radio frequency (RF) coils of the NMR magnet[14] (where electrolysis was not exhaustive) detected the rapid disappearance of all the peaks in the cyclic portion of the molecule due to rapid electron exchange with the cation radical.[4b]

In the ^{13}C NMR spectrum, the quaternary carbon shifts from 73.1 ppm in the neutral molecule up to 99.9 ppm in the cation, consistent with a decrease in electron density in the region of the quaternary carbon. Also, in the ^{13}C NMR spectrum, the cationic complex shows two bands in the carbonyl region (194.8 and 184.5 ppm) consistent with a quinoid complex and with the downfield band associated with the strongly electropositive carbon in the quinoid ring bonded to the chromanol oxygen (atom d in Figure 4). The ^1H NMR spectra also support an increase in positive charge in the region around the quaternary carbon, with all proton resonances in the vicinity of the

(13) Webster, R. D. *Electrochem. Commun.* **2003**, *5*, 6−11, and references therein.
(14) Webster, R. D. *Anal. Chem.* **2004**, *76*, 1603−1610.

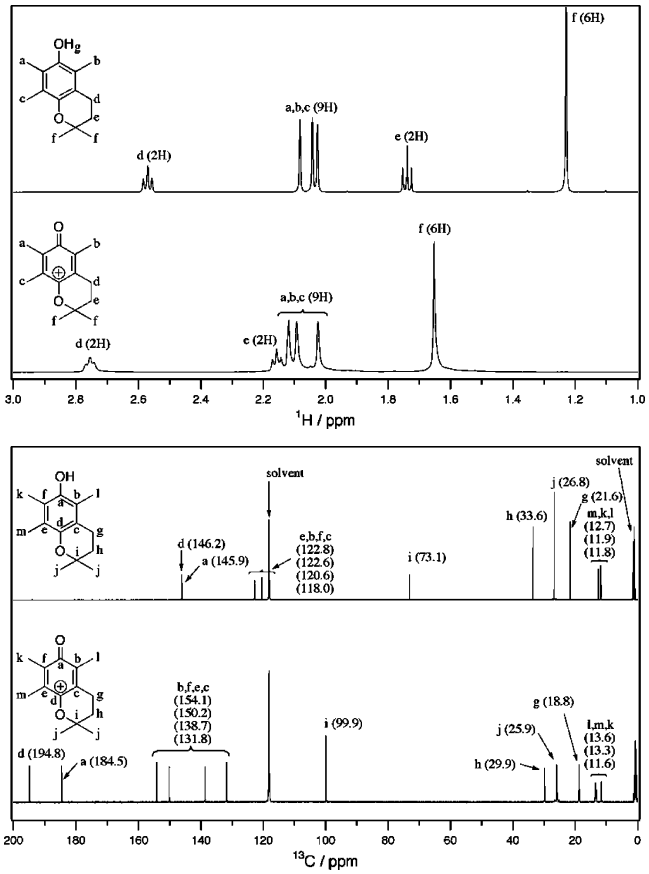

FIGURE 4. NMR spectra (500 MHz ^{1}H and 125.721 MHz ^{13}C) at 233 K in CD_3CN of 0.57 M (CH_3)α-TOH and its associated phenoxonium cation, (CH_3)α-TO^+, formed by reacting the starting material with 2 mol of $NOSbF_6$ at 233 K (eq 6). ^{1}H spectra represent 128 accumulated scans, and ^{13}C spectra represent 2000 accumulated scans.

nonaromatic chromanol ring shifting upfield. As expected, the OH resonance in the ^{1}H NMR spectrum of (CH_3)α-TOH at 5.4 ppm was missing from the spectrum of (CH_3)α-TO^+. A broad band occurred in the ^{1}H NMR spectrum of (CH_3)α-TO^+ at ca. 10 ppm at 233 K (and ca. 12 ppm at 298 K), consistent with the presence of the acidic byproduct, $[CD_3CNH]^+SbF_6^-$.

Extra peaks appeared in the ^{1}H and ^{13}C NMR spectra as the (CH_3)α-TO^+ solution was warmed to room temperature, although the phenoxonium cation could still be detected after several hours at 298 K. When 10 μL of water (∼1 M) was added to the NMR tube, the ^{1}H NMR peaks corresponding to (CH_3)α-TO^+ disappeared immediately and the NMR spectra became very complicated, indicating that multiple products were being formed (thin-layer chromatography (TLC) analysis also indicated that numerous products were formed) (Supporting Information Figure S5). Therefore, the decomposition of phenoxonium cations in CD_3CN containing low levels of water occurs by a mechanism more complicated than the simple hydrolysis mechanism depicted in eq 1. The NMR spectra of oxidized solutions of α-TOH and especially (COOH)α-TOH were not as clean as the spectra of (CH_3)α-TO^+ and indicated that some decomposition of the phenoxonium cation was occurring on the experimental timescale. The α-TO^+ and (COOH)α-TO^+

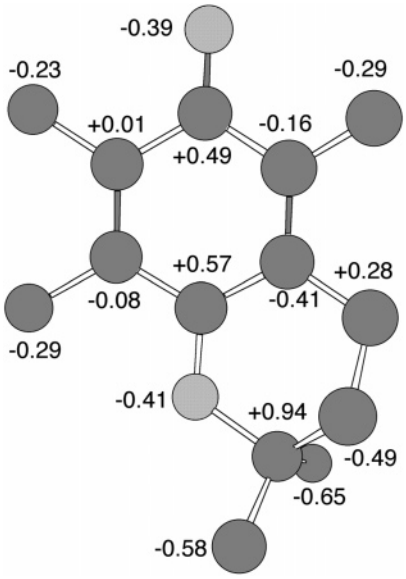

FIGURE 5. HF/6-31+G* potential-derived electrostatic charges for (CH_3)α-TO^+. Hydrogen atoms are omitted for clarity.

cations are possibly not as thermally stable in solution as (CH_3)α-TO^+, and thus, decomposition occurred while transferring the sample to the spectrometer. The ^{13}C NMR spectrum of α-TO^+ showed bands at 102.4, 187.6, and 195.1 ppm, in close agreement with the quaternary carbon and carbonyl-type resonances observed in the spectrum of (CH_3)α-TO^+. The phenoxonium cations are substantially more soluble in CH_3CN than their parent compounds (α-TOH and (COOH)α-TOH are soluble at ∼15 mM concentrations in CH_3CN, and (CH_3)α-TOH is soluble up to at least 1 M at 293 K) and are consequently difficult to precipitate from solution as pure compounds free from the acid byproduct. Furthermore, thermal and moisture instability have made additional purification and crystallization of the cations extremely difficult.

It is likely that other oxidizing agents will also produce the phenoxonium cations, providing they can be used in dry conditions. However, it was found that Ag^+ (used as $AgNO_3$ or $AgClO_4$) was not a sufficiently strong oxidant in CH_3CN to oxidize α-TOH to α-TO^+. The choice of the counteranion was also found to be important in stabilizing the phenoxonium cations. Cyclic voltammetry experiments indicated that the cation radical or phenoxonium ion were unstable in the presence of chloride (possibly due to homogeneous oxidation of the halide by α-$TOH^{+\bullet}$ or α-TO^+).

^{1}H and ^{13}C NMR predictions using fully empirical correlations usually provide an excellent match to experimental NMR spectra. However, empirical predictions of the NMR spectra of the phenoxonium cation were not productive because of the scarcity of data on related compounds (we are aware of no published NMR data on phenoxonium cations) and because of delocalization of the positive charge. Potential-derived charges (HF/6-31+G*) for each of the non-hydrogen atoms in the phenoxonium cation are shown in Figure 5. The assumption that the calculated ^{13}C NMR spectrum of the phenoxonium cation (Supporting Information Figure S6) is acceptable at the HF/6-31G* level of theory is supported by the accuracy of the theoretical spectrum of the starting phenol com-

pared to that of the experimental spectrum (compare Figure 4 and Supporting Information Figure S6). The theoretical calculations predict that the chemical shift of the quaternary carbon increases from 61.1 ppm (73.1 ppm experimental) in the neutral molecule up to 86.4 ppm (99.9 ppm experimental) in the cation. The theoretical calculations predict chemical shifts of 199.6 ppm (194.8 ppm experimental) and 173.5 ppm (184.5 ppm experimental) for the carbon atoms bonded to oxygen atoms in the phenoxonium cation.

2.4. Chemical Oxidation with $NOSbF_6$ in CH_2Cl_2. The addition of $NOSbF_6$ to α-TOH, (CH_3)α-TOH, and (COOH)α-TOH in pure CH_2Cl_2 resulted in the formation of dark-green colored solutions with electron paramagnetic resonance (EPR) experiments indicating the presence of paramagnetic compounds. The obtained EPR spectra of the three oxidized phenols in CH_2Cl_2 were similar, indicating that the structures of the radicals were closely related (Supporting Information Figure S7a), and were the same as the spectrum obtained by electrochemical oxidation of α-TOH in CH_3CN in the presence of CF_3SO_3H (that also produced green solutions).[4b] The radical in the green solutions had previously been assigned to α-$TOH^{+\bullet}$ on the basis of the observation that the signal intensity and stability increased as acid was added to the solution as a result of the equilibrium in eq 3 shifting toward the protonated species. The α-$TO^{\bullet}$ radical can be electrochemically formed by one-electron oxidation of the phenolate anion (Scheme 1)[5] but was not detected in this work (it has a substantially different EPR spectrum from the spectra assigned to the phenol cation radicals (Supporting Information Figure S7b)).[5b,11,15] The α-$TO^{\bullet}$ radical was not expected to be stable under the conditions used for this study because its low oxidation potential (∼+0.2 V vs Fc/Fc^+) necessitates that it will undergo immediate further oxidation with NO^+ to form α-TO^+ (Scheme 1) (no attempt was made at trapping the α-$TO^{\bullet}$ radical with spin markers). In contrast, α-$TOH^{+\bullet}$ cannot be oxidized until at least +1.4 V vs Fc/Fc^+ (Scheme 1);[4] therefore, it is stable in the presence of NO^+ and its concentration in solution is determined by K_{eq} in eq 3. The relative amount of cation radicals was difficult to quantify, but it is likely they exist together in solution with the phenoxonium cations because of the equilibrium constant in eq 3 shifting toward the protonated species in the low dielectric constant solvent CH_2Cl_2 (similar to that observed in acidified CH_3CN). The cation radicals are more intensely colored than the phenoxonium cations and so dominate the overall solution color (for α-$TOH^{+\bullet}$, $\lambda_{max} = 464$ nm and $\epsilon \geq 1.3 \times 10^4$ L cm^{-1} mol^{-1}).[4]

CV experiments performed on α-TOH and (CH_3)α-TOH in CH_2Cl_2 were similar on GC and Pt electrodes and clearly showed the presence of the cation radicals when the scan directions were reversed (that were not detected in pure CH_3CN) (Figure 6). On the forward scan, one anodic peak was detected at ∼ +0.5 V vs Fc/Fc^+ (similar to that in CH_3CN), and on the reverse scan, cathodic peaks were observed at ∼ +0.4 V (associated with the reduction of the cation radical) and at ∼ +0.15 V vs Fc/Fc^+ (associated with the reduction of the phenoxonium cation). The reverse peak at +0.4 V was larger in solutions containing (CH_3)α-TOH compared to those containing α-TOH, suggesting a higher proportion of the cation radical. Although the CV behavior in CH_2Cl_2 appeared simpler than that observed in CH_3CN, particularly at higher temperatures (in the sense that the voltammetry was very similar on both electrode surfaces in CH_2Cl_2), the longer-term bulk oxidation experiments were simpler in CH_3CN because the reaction proceeded quantitatively to the phenoxonium cation (as proven by the NMR and IR experiments). It was interesting to observe that the CV behavior of (COOH)α-TOH was significantly different from that of the two other phenols when the scan direction was reversed (in CH_3CN and CH_2Cl_2), but the bulk species produced by chemical oxidation were the same (as indicated by IR experiments).

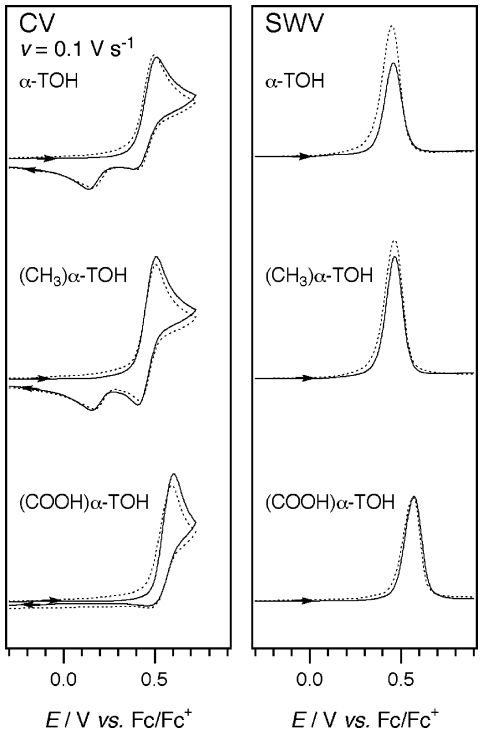

FIGURE 6. Voltammetric data for 2 mM substrates obtained at 293 K in CH_2Cl_2 with 0.2 M Bu_4NPF_6 at 1 mm diameter planar Pt (—) and GC (- - -) electrodes.

3. Conclusions

Chemical oxidation of α-TOH with the structurally similar nonnatural phenols (CH_3)α-TOH and (COOH)α-TOH with $NOSbF_6$ in CH_3CN at 233 K is a straightforward method for preparing the phenoxonium cations in high concentrations in solution in accordance with heterogeneous electrochemical electrolysis procedures.[4] The chemical oxidation reaction occurs in three steps in CH_3CN: initial one-electron oxidation to form the phenol cation radical, deprotonation of the cation radial to form the neutral radical, and further one-electron oxidation of the neutral radical to form the phenoxonium cation. When the oxidation reaction is conducted in the low dielectric constant solvent CH_2Cl_2, the deprotonation

(15) (a) Kohl, D. H.; Wright, J. R.; Weissman, M. *Biochim. Biophys. Acta* **1969**, *180*, 536−544. (b) Ozawa, T.; Hanaki, A.; Matsumoto, S.; Matsuo, M. *Biochim. Biophys. Acta* **1978**, *531*, 72−78. (c) Mukai, K.; Tsuzuki, N.; Ishizu, K.; Ouchi, S.; Fukuzawa, K. *Chem. Phys. Lipids* **1981**, *29*, 129−135. (d) Matsuo, M.; Matsumoto, S.; Ozawa, T. *Org. Magn. Reson.* **1983**, *21*, 261−264.

reaction is partially inhibited resulting in solutions containing the phenol cation radicals that are detectable by EPR spectroscopy. Therefore, direct oxidation of vitamin E in a lipophilic membrane could result in the formation of both α-$TOH^{+\bullet}$ and α-TO^+, depending on the dielectric properties of the medium. The formation of α-$TO^\bullet$ in a lipophilic membrane is more likely to involve a hydrogen atom abstraction mechanism rather than an oxidation mechanism, unless the oxidation occurs through the phenolate anion, α-TO^- (Scheme 1).

CH_3CN solutions containing each of the phenoxonium cations display three strong infrared absorbancies at 1670, 1649, and 1605 cm^{-1}. Theoretical calculations predict that the fundamental vibrational modes corresponding to the absorbancies are a C=O stretch, a symmetric C=C ring stretch, and an asymmetric C=C ring stretch. ^{13}C NMR spectroscopy experiments and theoretical calculations performed on (CH_3)α-TO^+ indicate that the positive charge is shared between the carbon atoms bonded to oxygen atoms and the quaternary carbon in the chromanol ring. The kinetic stability of the intermediate phenol cation radicals and neutral radicals (α-$TOH^{+\bullet}$ and α-$TO^\bullet$) does not appear to be an important prerequisite for the stability of the phenoxonium cations because α-$TO^\bullet$ is kinetically less stable than α-TO^+, especially at high concentrations. The crucial factor in the reversibility of the chemical transformation in eq 6 in CH_3CN is that, in contrast to most phenol cation radicals, the intermediate cation radical formed by the initial one-electron oxidation is only weakly acidic ($K_{eq} \sim K_a \sim 10^{-7}$ mol L^{-1}).

4. Experimental Section

4.1. Reagents. HPLC grade acetonitrile and analytical grade dichloromethane were dried and stored over calcium hydride (under nitrogen) and distilled immediately prior to use, and acetonitrile-d_3 (99.8% D) was stored over 4 Å molecular sieves under nitrogen. Chemical oxidation experiments were conducted using conventional vacuum-line techniques to ensure a moisture-free environment.

4.2. Apparatus. Solution-phase FTIR experiments were conducted utilizing a diamond composite attenuated total reflection (ATR) probe.[16]

4.3. Theoretical Calculations. Cyclic voltammetry simulations were performed using DigiSim 3.03.[17] Molecular orbital calculations were performed using a development version of the Q-Chem 2.1 software package[18] and the Spartan 04 software package.[19] Harmonic vibrational frequencies were calculated by Q-Chem using the EDF2/6-31+G* density functional model[20] and the SG-1 quadrature grid,[21] and no empirical scale factors were applied. NMR chemical shifts (without spin−spin coupling) were calculated by Spartan at the HF/6-31G* level using molecular structures optimized at the same level. Electrostatic potential maps and potential-derived atomic charges were computed by Spartan at the HF/6-31+G* level using structures optimized at the same level.

Acknowledgment. R.D.W. thanks the ARC for the award of a QEII Fellowship.

Supporting Information Available: Photograph showing typical red/orange color of phenoxonium cations. Solution-phase ATR-FTIR spectra obtained during the electrolysis of 2,6-di-*tert*-butyl-4-methoxyphenol and solid-state FTIR spectra of (COOH)α-TO^+. Theoretical normal modes of vibration of (CH_3)α-TO^+. ^1H NMR spectra showing the decomposition of (CH_3)α-TO^+. Theoretical ^{13}C NMR spectra of (CH_3)α-TOH and (CH_3)α-TO^+. EPR spectra of cation radicals produced by chemical oxidation of the phenols in CH_2Cl_2. Summary of results from theoretical calculations (Cartesian coordinates, no. of imaginary frequencies, and total energies). This material is available free of charge via the Internet at http://pubs.acs.org.

JO0517951

(16) Webster, R. D. *J. Chem. Soc., Perkin Trans. 2* **2002**, 1882−1888.

(17) (a) *DigiSim*;Bioanalytical Systems, Inc. (BAS): West Lafayette, IN. (b) Rudolph, M.; Reddy, D. P.; Feldberg, S. W. *Anal. Chem.* **1994**, *66*, 589A−600A.

(18) Kong, J.; White, C. A.; Krylov, A. I.; Sherrill, C. D.; Adamson, R. D.; Furlani, T. R.; Lee, M. S.; Lee, A. M.; Gwaltney, S. R.; Adams, T. R.; Ochsenfeld, C.; Gilbert, A. T. B.; Kedziora, G. S.; Rassolov, V. A.; Maurice, D. R.; Nair, N.; Shao, Y.; Besley, N. A.; Maslen, P. E.; Dombroski, J. P.; Daschel, H.; Zhang, W.; Korambath, P. P.; Baker, J.; Byrd, E. F. C.; Van Voorhis, T.; Oumi, M.; Hirata, S.; Hsu, C.-P.; Ishikawa, N.; Florian, J.; Warshel, A.; Johnson, B. G.; Gill, P. M. W.; Head-Gordon, M.; Pople, J. A. *J. Comput. Chem.* **2000**, *21*, 1532−1548.

(19) *Spartan 04 for Macintosh*; Wavefunction Inc.: Irvine, CA.

(20) Lin, C. Y.; George, M. W.; Gill, P. M. W. *Aust. J. Chem.* **2004**, *57*, 365−370.

(21) Gill, P. M. W.; Johnson, B. G.; Pople, J. A. *Chem. Phys. Lett.* **1993**, *209*, 506−512.